Bulletin of Entomological Research

cambridge.org/ber

RNA *N6*-methyladenosine of *DHAPAT* and *PAP* involves in regulation of diapause of *Bombyx mori* via the lipid metabolism pathway

Yan-Hua Chen[1,2,*], Tao Jiang[3,*], Ayinuer Yasen[1,2], Bing-Yan Fan[1,2], Juan Zhu[1,2], Mei-Xian Wang[1,2] and Xing-Jia Shen[1,2]

[1]Jiangsu Key Laboratory of Sericultural Biology and Biotechnology, College of Biotechnology, Jiangsu University of Science and Technology, Zhenjiang, Jiangsu 212100, China; [2]Key Laboratory of Silkworm and Mulberry Genetic Improvement, Ministry of Agriculture and Rural Affairs, Sericulture Research Institute, Chinese Academy of Agricultural Sciences, Zhenjiang, Jiangsu 212100, China and [3]Silkworm Egg Institute of Jiangsu Province, Wuxi, Jiangsu 214000, China

Research Paper

*These authors contributed equally to this work.

Cite this article: Chen Y-H, Jiang T, Yasen A, Fan B-Y, Zhu J, Wang M-X, Shen X-J (2023). RNA *N6*-methyladenosine of *DHAPAT* and *PAP* involves in regulation of diapause of *Bombyx mori* via the lipid metabolism pathway. *Bulletin of Entomological Research* **113**, 665–675. https://doi.org/10.1017/S0007485323000330

Received: 2 March 2023
Revised: 14 March 2023
Accepted: 3 July 2023
First published online: 9 August 2023

Keywords:
Bombyx mori; *DHAPAT*; diapause; lipid metabolism; *PAP*; post-transcriptional regulation; RNA *N6*-adenosine methylation; YTHDF3

Corresponding author:
Xing-Jia Shen; Email: shenxjsri@163.com

Abstract

Environment-induced epigenetics are involved in diapause regulation, but the molecular mechanism that epigenetically couples nutrient metabolism to diapause regulation remains unclear. In this study, we paid special attention to the significant differences in the level of *N6*-adenosine methylation (m^6A) of dihydroxyacetone phosphate acyltransferase (*DHAPAT*) and phosphatidate phosphatase (*PAP*) genes in the lipid metabolism pathway of the bivoltine silkworm (*Bombyx mori*) strain Qiufeng developed from eggs incubated at a normal temperature (QFHT, diapause egg producer) compared to those from eggs incubated at a low temperature (QFLT, non-diapause egg producer). We knocked down *DHAPAT* in the pupal stage of the QFLT group, resulting in the non-diapause destined eggs becoming diapausing eggs. In the *PAP* knockdown group, the colour of the non-diapause destined eggs changed from light yellow to pink 3 days after oviposition, but they hatched as normal. Moreover, we validated that YTHDF3 binds to m^6A-modified *DHAPAT* and *PAP* mRNAs to promote their stability and translation. These results suggest that RNA m^6A methylation participates in the diapause regulation of silkworm by changing the expression levels of *DHAPAT* and *PAP* and reveal that m^6A epigenetic modification can be combined with a lipid metabolism signal pathway to participate in the regulation of insect diapause traits, which provides a clearer image for exploring the physiological basis of insect diapause.

Introduction

Diapause is a genetic characteristic gradually formed in the long evolutionary process of insects to avoid adverse living environments for continuation and to improve population abundance. Insect diapause is determined by genes (Gupta, 1991; Kitagawa *et al.*, 2005) controlled by hormones and specific external stimuli, such as temperature, photoperiod and nutrition (Fischman *et al.*, 2017; Pitts-Singer, 2020; Süess *et al.*, 2022). Before entering the diapause period, it is necessary to isolate additional metabolic energy by sensing the shift of environmental conditions (Hand *et al.*, 2011; Lehmann *et al.*, 2016). Even if the environment returns to favourable conditions, diapause continues until the procedure is terminated (Taylor, 1987; Koštál, 2006). In diapause preparation, a series of physiological changes occur in insects, including the specific accumulation and transformation of lipids, proteins, carbohydrates and other nutrients, to ensure the survival of diapausing individuals under adverse and energy shortage conditions. Compared with the non-diapause generation or development stage, the expression profile of genes related to development stagnation, metabolic inhibition and stress resistance increases in diapausing insects (Amsalem *et al.*, 2015; Popović *et al.*, 2015; Wadsworth and Dopman, 2015). Lipids are the main energy resource to cope with periods of food deprivation, providing nutrients, transforming other nutrients and serving as cryoprotective substances through lipid metabolism for diapausing insects (Hahn and Denlinger, 2007; Izumi *et al.*, 2007; Arrese and Soulages, 2009; Vukašinović *et al.*, 2018). Transcriptomics have promoted an understanding of the molecular regulation of insect diapause, and several studies have identified hundreds of diapause-related genes, including in the nutrition metabolism pathway (Poupardin *et al.*, 2015; Kang *et al.*, 2016; Ragland and Keep, 2017). Metabonomic studies have shown that diapausing insects store more lipids than non-diapausing individuals, and metabolites related to lipid metabolism during diapause are significantly reduced (Li *et al.*, 2015; Batz and Armbruster, 2018). The preservation of lipids during diapause is manifested by the downregulation of genes related to lipid catabolism

(Reynolds *et al*., 2012). However, the proximal mechanism leading to changes in lipid metabolism during diapause is still unclear.

Epigenetics are phenotypic inheritance mechanisms independent of genomic changes that are regulated by multiple environmental signals and play an important role in regulating diapause-related gene expression (Bonasio *et al*., 2010; Rando, 2012). The expression of heterochromatin protein 1 (HP1) in diapausing pupae of *Sarcophaga bullat* is downregulated by nearly 50% compared with non-diapausing pupae, while HP1 can interact with histone demethylase dKDM4A and participate in the regulation of developmental plasticity and lipid metabolism (Meister *et al*., 2011; Reynolds, 2017). Analysis of DNA methylation and the transcriptome of silkworm (*Bombyx mori*) showed that diapause eggs have higher DNA methylation modification in lipid metabolism-related genes than developing eggs after diapause termination (Li *et al*., 2020). Moreover, miRNAs, another important endogenous regulating factor, are variously expressed in diapausing and non-diapausing insects, and their target genes affect the regulation of diapause-related processes, such as the lipid metabolism pathway (Ragland *et al*., 2010; Batz *et al*., 2017; Reynolds *et al*., 2017). These results indicate that epigenetic modification is involved in the regulation of lipid metabolism to affect insect diapause, but the role of m^6A methylation regulating insect diapause coupled with lipid metabolism is still unknown. In human and other animal studies, m^6A methylation has a significant effect on the regulation of lipid metabolism (Gebeyew *et al*., 2022; Wang *et al*., 2022). The expression level of demethylase FTO is negatively correlated with the m^6A level, and *FTO* knockout affects lipid metabolism, leading to an increase in energy consumption (Boissel *et al*., 2009; Smemo *et al*., 2014; Wang *et al*., 2015; Takemoto *et al*., 2021). Decreasing the m^6A abundance of peroxisome proliferator-activated receptor α (*PPaRα*) in mice leads to reduced cell lipid accumulation and affects the regulation of the circadian rhythm in lipid metabolism (Zhong *et al*., 2018). These results indicate that m^6A methylation modification of RNA is involved in lipid metabolism in animals. However, the regulatory mechanism of lipid metabolism in diapausing insects remains unclear.

To advance the study of the epigenetic regulation of the developmental pathways of Lepidopteran model organisms, this paper sought to study the egg diapause phenotype of the model silkworm (*B. mori*). Diapause traits of silkworm are induced by environmental signals, in which epigenetics play an important role. Studies have shown that m^6A methylation is involved in the expression regulation of diapause-related genes, and m^6A abundance in the early embryonic development stage of diapausing eggs is higher than that of non-diapausing eggs (Jiang *et al*., 2019). Reader protein YTHDF3 of the m^6A modification system is involved in diapause regulation of bivoltine silkworm by altering the expression of *Cyp307a1* and *Cyp18a1* genes in the pathway of ecdysone synthesis (Chen *et al*., 2022), but it cannot completely change the diapause fate of silkworm eggs, implying that m^6A may regulate diapause in multiple ways. The complex and diverse utilization mechanism of nutrients is a typical characteristic of silkworm in regulating diapause in response to environmental signals, but the relationship between epigenetics and the molecular mechanism of nutrient metabolism is unknown. Based on analysis of previous m^6A methylation sequencing data, we found a significant difference in the m^6A methylation modification of dihydroxyacetone phosphate acyltransferase (*DHAPAT*) and phosphatidic acid phosphatase (*PAP*) genes in the 3 day pupal stage between the non-diapausing egg producer (QFLT) group and the diapausing egg producer (QFHT) group; the expression levels of two genes in the QFLT group were higher than the QFHT group. Triacylglycerol, a product of lipid metabolism, releases fatty acids into the tricarboxylic acid cycle through lipolysis to produce energy. Therefore, we verified that m^6A mediates *DHAPAT* and *PAP* methylation to change the expression of *DHAPAT* and *PAP* and then participates in the diapause regulation of silkworm through the lipid metabolism pathway and tricarboxylic acid cycle. This study clarified the regulation of diapause traits of silkworm by epigenetic coupling lipid metabolism and deepened the understanding of insect metamorphosis and diapause mechanisms, and may provide new insights on how to better utilize insects as resources and for pest management.

Materials and methods

Animals

The materials used in this experiment were univoltine silkworm (*B. mori*) strain AK4, bivoltine strain Qiufeng (QF), multivoltine with diapause strain 'SH' and multivoltine of non-diapause strain Nistari. According to the principle that diapause of the bivoltine strain is regulated by environmental factors, mainly temperature and light, diapause-terminated silkworm egg batches (one batch produced by one female moth) of QF were divided into two semi-batch groups, one of which was incubated at 17°C in darkness (QFLT) to produce non-diapause eggs. To produce diapause eggs of QF, the other sample group was incubated at 25°C under a natural day/night cycle (QFHT) 15 days later for hatching on the same day with QFLT. After hatching, the larvae of both groups were raised with fresh mulberry leaves under 25°C with a relative humidity of 80 ± 5% under natural light. Ovary tissue and fat body were taken for the samples from the 1st day to 6th day of pupal stage and then stored at −80°C for later use. Five pupae were taken as one sample, and each sample was replicated in three groups.

Reagents

The pFastBac-dual vector, pGL-*A3*-*luc*-sv40 vector and DH10Bac were provided by the Key Laboratory of Sericultural Research Institute, Chinese Academy of Agri-cultural Sciences (CAAS). Primer synthesis and sequencing were performed by Sangon Biotech (Hangzhou, China). MeRIP kit (No: P-9018) is purchased from Epigentek Company (Guangzhou, China). Actinomycin D was purchased from Macklin (Shanghai, China). TC-100 was purchased from Applichem (Germany), and foetal bovine serum (FBS) was purchased from Corning (USA). Dual-Luciferase Reporter Assay System was purchased from Promega. The plasmid extraction kit, RT-PCR kit and SYBR Green PCR kit were obtained from Vazyme Company.

Cell culture

*Bm*N cells originated from *B. mori* ovary were cultured in TC-100 insect culture medium supplemented with 10% FBS and 1% penicillin streptomycin. Plasmid transfection was performed with Effectene Transfection Reagent (Qiagen) according to the manufacturer's protocol. After 6 h, the medium was replaced with a culture medium containing 10% FBS for 48 h to observe fluorescence or collect cells.

Quantification of mRNA methylation with m^6A-IP and RT-qPCR

The kit was used to enrich m^6A modified gene according to the instructions, and then RT-qPCR method was used to quantify

https://doi.org/10.1017/S0007485323000330 Published online by Cambridge University Press

Table 1. Primers

Primer name	Sequence	Primer purpose
PAP-F	ATGGACAGAACCGAGAGAAAA	pFastBac Dual
PAP-R	TCAGACTTGGACGCGAGGGTG	pFastBac Dual
DHAPAT-F	ATGGGACTAGATAAAAAATTAC	pFastBac Dual
DHAPAT-R	TCACAGTCTAGACGAGGTTCT	pFastBac Dual
PAPA-T7F	GGATCCTAATACGACTCACTATAGGTCGTGATGTCAACCGAACAT	dsRNA
PAP-R	AGATTCATCCACCCAACAGC	dsRNA
PAP-F1	TCGTGATGTCAACCGAACAT	dsRNA
PAP-T7R	GGATCCTAATACGACTCACTATAGGAGATTCATCCACCCAACAGC	dsRNA
DHAPAT-T7F	GGATCCTAATACGACTCACTATAGGTACCATAGTGCCCGTGAACA	dsRNA
DHAPAT-F	TACCATAGTGCCCGTGAACA	dsRNA
DHAPAT-R	ACCCAGACCACTTCAACGAC	dsRNA
DHAPAT-T7R	GGATCCTAATACGACTCACTATAGGACCCAGACCACTTCAACGAC	dsRNA
PAP-F	TCGTAACATCGATGCAGTGAAA	Real-time PCR
PAP-R	TCGCAGTATCATTTTAGAATCTCG	Real-time PCR
DHAPAT-F	AATTTCGTTGATATCCTAGAGCCGA	Real-time PCR
DHAPAT-R	GGCGAATAGATTTTATCTAAGGCCA	Real-time PCR
PAP-RT1	CCATCTTTAAACTTAATAG	Reverse transcription
PAP-RT2	AGAGTTTAATGTACAACAATAAA	Reverse transcription
PAP-RT3	CGCGAATTCGTTTTTCTCTCGGTT	Reverse transcription
DHAPAT-RT1	ATGTAGCGAAATGTGTCGGAT	Reverse transcription
DHAPAT-RT2	CTCGGCTCTAGGATATCAACGAAA	Reverse transcription
DHAPAT-RT3	TCTAAGGCCATAGTTTTTAC	Reverse transcription
PAP-RT-F	TCGCTCTTGTGTTTCTGAACG	Real-time PCR
PAP-RT-R	ACTTTTCACTGCATCGATGTTACG	Real-time PCR
DHAPAT-RT-F	TCTGTCGTGATGAGATAGTGTGT	Real-time PCR
DHAPAT-RT-R	TCACTTCCTCACTCATTTTGAATTT	Real-time PCR
PAP-wtF	GTTGTACATTAAACTCTGGAC	pGL-A3-luc
PAP-wt/mutR	ATCGTCGCAGAAGAACACCA	pGL-A3-luc
PAP-mutF	GTTGTACATTAAACTCTGGTC	pGL-A3-luc
DHAPAT-wtF	GCCGAGAAGGACTGAATCCG	pGL-A3-luc
DHAPAT-wtR	ACCTGTCCTGGTGCTCTCA	pGL-A3-luc
DHAPAT-mutF	GCCGAGAAGGTCTGAATCCG	pGL-A3-luc

the methylation changes of the target gene. The mRNA extracted from the sample and the m^6A capture antibody combined with beads were incubated in the buffer for 90 min, and the RNA sequences containing both ends of the m^6A target region were cleaved in nuclear digestion enhancer and cleavage enzyme mix reagents. Then, the enriched RNA was released, purified and eluted through RNA binding beads, and the samples were stored at −20 °C. The enrichment of m^6A in each sample was analysed by RT-qPCR.

Construction of the baculovirus expression system

Recombinant baculoviruses BmBacJS13-*egfp* and BmBacJS13-*egfp-YTHDF3* were constructed earlier in this project (Chen *et al.*, 2022). Primers of *DHAPAT* and *PAP* were designed (table 1). The cloned *DHAPAT* and *PAP* were inserted between *Not* I and *Xho* I and *Sal* I and *Hind* III at the downstream of the vector pFastBac Dual-*egfp*, respectively. The constructed pFastBac Dual-egfp-*DHAPAT* and pFastBac Dual-*egfp-PAP* plasmids were transformed into DH10Bac competent cells to construct recombinant baculoviruses BmBacJS13-*egfp-DHAPAT* and BmBacJS13-*egfp-PAP*.

dsRNA synthesis

The dsRNA primers of *DHAPAT* and *PAP* were designed according to the NCBI database and the online software SnapDragon – dsRNA design (table 1). After polymerase chain reaction with

https://doi.org/10.1017/S0007485323000330 Published online by Cambridge University Press

these two pairs of primers, the template of dsRNA was prepared with T7Megascript Kit (NEB) to synthesize double-stranded dsRNA and achieve gene knockdown.

In vivo *injection*

Two microlitres of dsRNA at a concentration of 2500 ng μl^{-1} were injected into 2nd day pupae of QFLT (none-diapause egg producer) with a microinjector. The injected pupae were preserved at 25℃ until eclosion. Then, females were mated with males for 6 h, and the separated females were put on an egg card to produce eggs for phenotypic observation, including egg colour, size and other traits related to diapause.

RNA immunoprecipitation (RIP)

Cells infected with BmBacJS13-*egfp* and BmBacJS13-*egfp-YTHDF3* were washed with PBS and then collected and centrifuged. The cells were then suspended in the cell lysate with protease inhibitor and ribonuclease inhibitor and incubated with 30 min on ice. Then, 1.5 µg of EGFP antibody or control IgG was conjugated to protein A/G beads and incubated at 4℃ for 6 h, washing for three times and then overnight incubation in RIP buffer (5 mM EDTA, 150 mM KCl, 25 mM Tris (pH 7.4), 1× protease inhibitor, 0.5 mM DTT, 0.5% NP40, 100 U ml^{-1} ribonuclease inhibitor) at 4°C. After washing for three times, resuspension at 100 µl PBS and 30 µg of protease K, digested at 37°C for 15 min. RNA was extracted with TRIzol reagent purchased from TaKaRa.

RNA isolation and quantitative RT-PCR analysis

After RNA was extracted with TRIzol reagent, reverse transcription was carried out with reverse transcription kit according to the requirements of manufacturers, and the expression level of related genes was quantitatively analysed by Power SYBR Green Master Mix. The primers are shown in table 1.

mRNA stability assay

The cultured BmN cells were seeded into a six-well plate at density about 60% (cell inoculum density 2×10^5 ml). After culture at 27℃ for 12 h, the collected baculoviruses were infected with BmN cells for YTHDF3 overexpression. Then, the transcription was blocked with 5 µg ml^{-1} actinomycin D, and the total RNA was collected at different time points, and the stability of target RNA was analysed by RT-qPCR. Since actinomycin D treatment results in transcription stalling, the change in mRNA concentration at a given time (dC/dt) is proportional to the constant of mRNA decay (K) and mRNA concentration (C), leading to the following equation: $dC/dt = -KC$, thus the mRNA degradation rate K was estimated by: $\mathrm{Ln}(C/C0) = -Kt$, to calculate the mRNA half-life ($t1/2$). When 50% of mRNA is decayed ($C/C0 = 1/2$), the equation was: $\mathrm{Ln}\ (1/2) = -Kt1/2$.

m^6A site validation

The peak obtained by sequencing was used to predict the m^6A methylation site by the software SRAMP (a sequence-based N6-methyladenosine (m^6A) modification site predictor). According to the difference in the transcription of m^6A methylation sites by the *Bst* I enzyme, reverse transcription primers were designed (table 1), and RT-qPCR site verification was performed (Castellanos-Rubio *et al.*, 2019).

Dual-luciferase reporter assay

Wild-type (wt) and point-mutant (A-T) primers of *DHAPAT* and *PAP* genes were designed respectively (table 1), and PCR products were connected to pMD19-T for sequencing verification. The wild-type and mutation sequence of *DHAPAT* and *PAP* genes containing m^6A methylation modification site were cloned into *Nco* I site of pGL-A3-luc plasmid to construct plasmids pGL-*A3-DHAPAT-wt/mut*-luc-sv40 and pGL-*A3-PAP-wt/mut-luc*-sv40, respectively. BmN cells were inoculated in triplicate in 24-well plates and infected with BmBacJS13-*egfp-YTHDF3* virus. Seventy-two hours later, according to the supplier's instructions, firefly luciferase (Fluc) and Renilla luciferase (Rluc) activity were measured using Dual-Luciferase Reporter Assay System.

Statistical analysis

SPSS 22.0 software was used for the analysis of the significant difference between treatments. All experiments were reproduced at least three times in separate and independent replicates. Statistical comparisons were performed by using *t*-tests (two tailed) as indicated in the figure legends. The data are presented as the mean ± standard deviation (SD). The * represents $P \leq 0.05$ difference, ** represents $P \leq 0.01$ significant difference, ***represents $P \leq 0.001$ extremely significant difference.

Results

DHAPAT *and* PAP *involves in the regulation of diapause in* B. mori

To explore the effects of *DHAPAT* and *PAP* on diapause in *B. mori*, the *DHAPAT* and *PAP* genes in 2-day-old pupae of the QFLT group were knocked down. The synthesized *dsDHAPAT* and *dsPAP* were transfected separately into *Bm*N cells at a rate of 500, 800, 1200 and 2000 ng per well. At 12, 24, 48 and 72 h post-transfection, the cells were collected for qPCR. *dsDHAPAT* and *dsPAP* showed interference effects, and the best efficiency was obtained at 48 h at 800 ng (fig. 1a, b).

Moreover, *dsDHAPAT* and *dsPAP* were injected separately into 2-day-old pupae of QFLT, and *dsEGFP*-injected pupae served as a control. After eclosion, the female moths were mated with males to produce eggs. Compared with the *dsEGFP* control, which laid non-diapausing eggs, all female moths from *dsDHAPAT*-treated pupae laid diapause eggs, while the female moths from *dsPAP*-treated pupae still laid non-diapausing eggs and hatched normally, only to turn pink in egg colour 3 days after oviposition (fig. 1c–e). These results indicate that *DHAPAT* and *PAP* have a certain regulation function in the lipid metabolism pathway for diapause of bivoltine silkworm strains.

Transcriptional expression profile of DHAPAT *and* PAP

Total RNAs were extracted from ovaries and fat bodies of *B. mori* strains AK4, QF (QFHT, QFLT), SH and Nistari at the pupal stage from 1 to 6 days. RT-qPCR showed that *DHAPAT* expression in the ovarian tissue of different *B. mori* strains was similar and stable from the 1st to the 5th day of pupae. The expression level of the non-diapausing egg producer (QFLT) and Nistari

https://doi.org/10.1017/S0007485323000330 Published online by Cambridge University Press

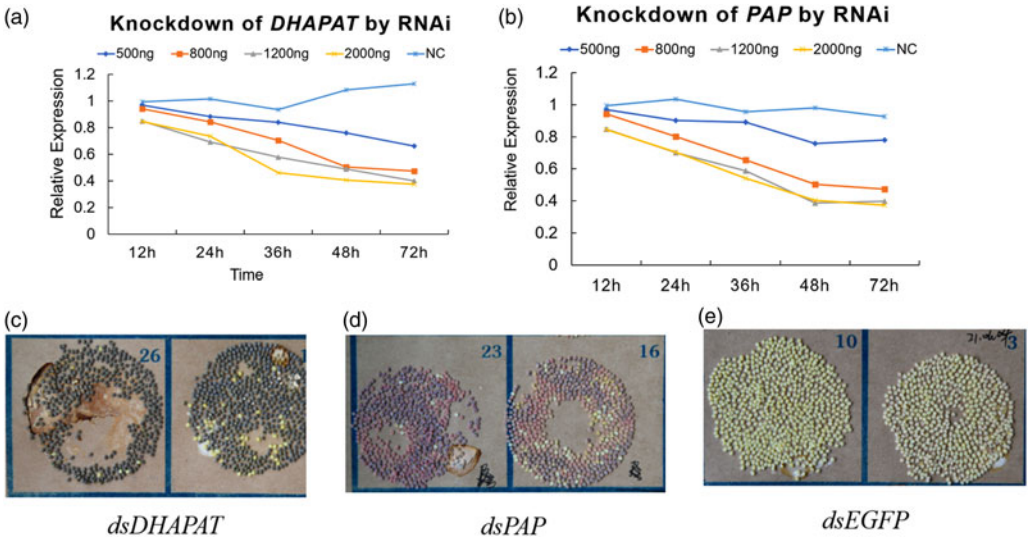

Figure 1. *DHAPAT* and *PAP* regulate *B. mori* diapause. (a) Knockdown of *DHAPAT* by RNAi in cells. (b) Knockdown of *PAP* by RNAi in cells. (c) Diapause eggs laid by moths from *DHAPAT* knockdown pupae of none-diapause producer group. (d) None-diapause eggs in pinkish colour laid by moths from *PAP* knockdown pupae of none-diapause producer group. (e) Eggs of the control are in light yellow.

was still stable on the 6th day, while the expression level of diapausing egg producers AK4 and QFHT and mixture producer (laying non-diapausing eggs mixed with diapausing eggs) of SH obviously varied (fig. 2a). In the fat body, the expression levels of SH and AK4 in pupae varied significantly, and the expression in QFLT and Nistari remained stable (fig. 2b). From 2 to 72 h in the embryonic developmental stage of eggs, *DHAPAT* expression showed a steady upward trend in all tested strains (fig. 2c).

Quantitative analysis showed that *PAP* expression in the ovaries of QFLT and SH remained stable, while the others revealed a downward trend (fig. 2d). The fat bodies of the above *B. mori* strains were relatively stable, but the expression level of the multivoltine *B. mori* strains was relatively low (fig. 2e). *PAP* expression in eggs of the early embryonic stage also showed a relatively stable trend in all strains, but it was generally lower in multivoltine strains (Nistari and SH) and higher in the QFHT and QFLT groups (fig. 2f). These results revealed that the expression levels of *DHAPAT* and *PAP* differ from the voltinism of *B. mori*, indicating that *DHAPAT* and *PAP* play important roles in diapause regulation and development of embryos in *B. mori*.

m^{6}A methylation level of DHAPAT *and* PAP *in the QFHT and QFLT groups*

Employing m^{6}A immunoprecipitation and RT-qPCR techniques, the m^{6}A methylation levels of the pupal ovaries and eggs of QFHT and QFLT were analysed. m^{6}A-modified *DHAPAT* increased from 1 to 6 days in the pupal stage in the ovaries of the QFLT group but decreased slowly in QFHT (fig. 3a). In the eggs, m^{6}A-modified *DHAPAT* in QFLT increased slowly, but the expression level in QFHT showed a significant downward trend from 24 to 72 h (fig. 3b).

Similarly, m^{6}A methylation level analysis of *PAP* showed that m^{6}A-modified *PAP* expression presents an upward trend in the QFLT group but a downward trend in QFHT after the 3rd day of pupae (fig. 3cC). In QFHT and QFLT eggs, the expression levels were basically the same within 36 h and began to increase after 48 h at different speeds, leading to a significantly higher expression level in QFLT than in QFHT (fig. 3d).

This analysis showed that there was a significant difference in the m^{6}A methylation levels of *DHAPAT* and *PAP* between the QFLT and QFHT groups, and the modification rate of the QFLT group was higher than that of the QFHT group. Our previous sequencing results showed that there was a higher methylation modification in QFLT, which is consistent with this result (Chen *et al.*, 2023).

YTDHF3 recognizes m^{6}A-modified DHAPAT *and* PAP

To explore the effect of m^{6}A modification on the expression level of *DHAPAT* and *PAP*, the constructed vectors BmBacJS13-*egfp-DHAPAT* and BmBacJS13-*egfp-PAP* were expressed in BmN cells, and fluorescence was observed under a microscope 4 days later. *DHAPAT* and *PAP* were localized in the cytoplasm (fig. 4a). According to the types of reader proteins found in *B. mori* and related studies, we speculate that YTHDF3 located in the cytoplasm is a potential reader of these two genes. Expression vectors BmBacJS13-*egfp* and BmBacJS13-*egfp-YTHDF3* were transfected into BmN cells and collected 2 days post-transfection for RNA immunoprecipitation with the EGFP and IgG antibodies, and the pulled RNAs were quantitatively analysed using RT-qPCR. The binding amount of *DHAPAT* and *PAP* in the overexpressed BmBacJS13-*egfp-YTHDF3*/EGFP antibody group was significantly higher than that in the control groups BmBacJS13-*egfp*/EGFP antibody and BmBacJS13-*egfp-YTHDF3*/IgG antibody (fig. 4b), indicating that YTHDF3 recognized and bound the m^{6}A methylation sites of *DHAPAT* and *PAP*.

The collected viruses of overexpressing BmBacJS13-*egfp-DHAPAT* and BmBacJS13-*egfp-PAP* were injected into 2-day-old pupae to observe the phenotype of egg colour after eclosion and mating. The overexpression of *DHAPAT* and *PAP* had no significant effect on the diapause phenotype.

YTHDF3 mediates DHAPAT *mRNA translation in the lipid metabolism pathway*

To explore how YTHDF3 regulates *DHAPAT* expression, the stability of *DHAPAT* mRNA was tested by *YTHDF3* overexpression

https://doi.org/10.1017/S0007485323000330 Published online by Cambridge University Press

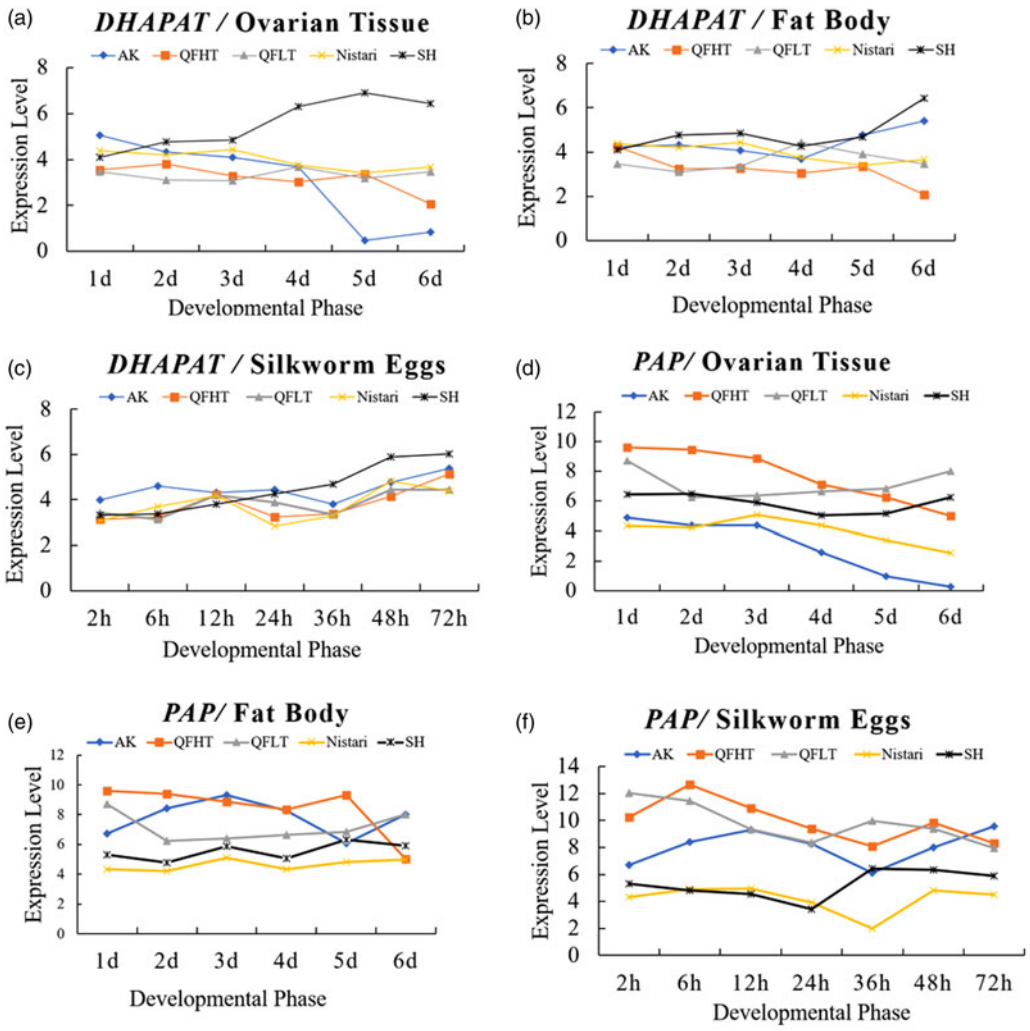

Figure 2. Expression profile of *DHAPAT* and *PAP* in ovary, fat body and early embryonic stage of different voltine *B. mori* strains. (a), (b) and (c) *DHAPAT* expression level in the ovary and fat body during pupa and early embryonic stage of eggs. (d), (e) and (f) *PAP* expression level in the ovary and fat body during pupa and early embryonic stage of eggs. Different strains are represented by colours: AK4(blue), QFHT (orange), QFLT (grey), SH (black) and Nistari (yellow). 1, 2, 3, 4, 5 and 6 d indicate the first to sixth day of pupal stage. 2, 6, 12, 24, 36, 48 and 72 h indicate the 2nd to 72nd hour of eggs after laying.

and actinomycin D inhibition in the cells. Compared with the control group, the half-life of *DHAPAT* in the experimental group was significantly increased, indicating that YTHDF3 affected the stability of *DHAPAT* mRNA and promoted the stability of the molecule (fig. 5a). To further investigate whether m^6A mediates the regulation of *DHAPAT* by YTHDF3, we used catRAPID software to predict the potential binding sites of YTHDF3 with *DHAPAT*. Then, the sequencing peak was predicted using SRAMP software, and two methylation sites were obtained. RT-qPCR showed that the m^6A modification site of *DHAPAT* was A (293), which is the binding region of YTHDF3 (fig. 5b, c). To validate this, we designed wild-type and mutant (A-T) primers (table 1) for this site to clone the correct and mutated sequences and construct a dual-luciferase gene reporter plasmid, respectively (fig. 5d). Then, the constructed wt, mutant and blank control plasmids were transfected into BmN cells. The results showed that the luciferase activity of wt *DHAPAT* was significantly higher than that of the mutant and the blank control, indicating that YTHDF3 promoted the expression of *DHAPAT* mRNA, while the expression level of the mutant was similar to that of the blank control, indicating that YTHDF3 has no regulatory effect on the mutated *DHAPAT* (fig. 5e). This demonstrated that the m^6A modification site of *DHAPAT* was correct. The quantitative results showed that the expression level of *DHAPAT* mRNA in the *wt* group was significantly higher than in the two control groups under YTHDF3 overexpression. Although *DHAPAT* could not be modified by m^6A or recognized by YTHDF3 and its mRNA level was also at a high level in the mutant group, it was significantly lower than that in the wt group (fig. 5f). This verified that YTHDF3 recognizes and binds the m^6A site of *DHAPAT* mRNA, increasing the stability of *DHAPAT* and promoting its translation.

YTHDF3 mediates PAP *mRNA translation in the lipid metabolism pathway*

Similarly, to explore the regulatory effect of YTHDF3 on *PAP*, the stability of *PAP* mRNA was tested. *PAP* mRNA stability was significantly increased under YTHDF3 overexpression (fig. 6a). Using SRAMP software, two methylation modification sites were predicted in *PAP* mRNA. RT-qPCR verification showed that A (161) was one methylation modification site (fig. 5b).

https://doi.org/10.1017/S0007485323000330 Published online by Cambridge University Press

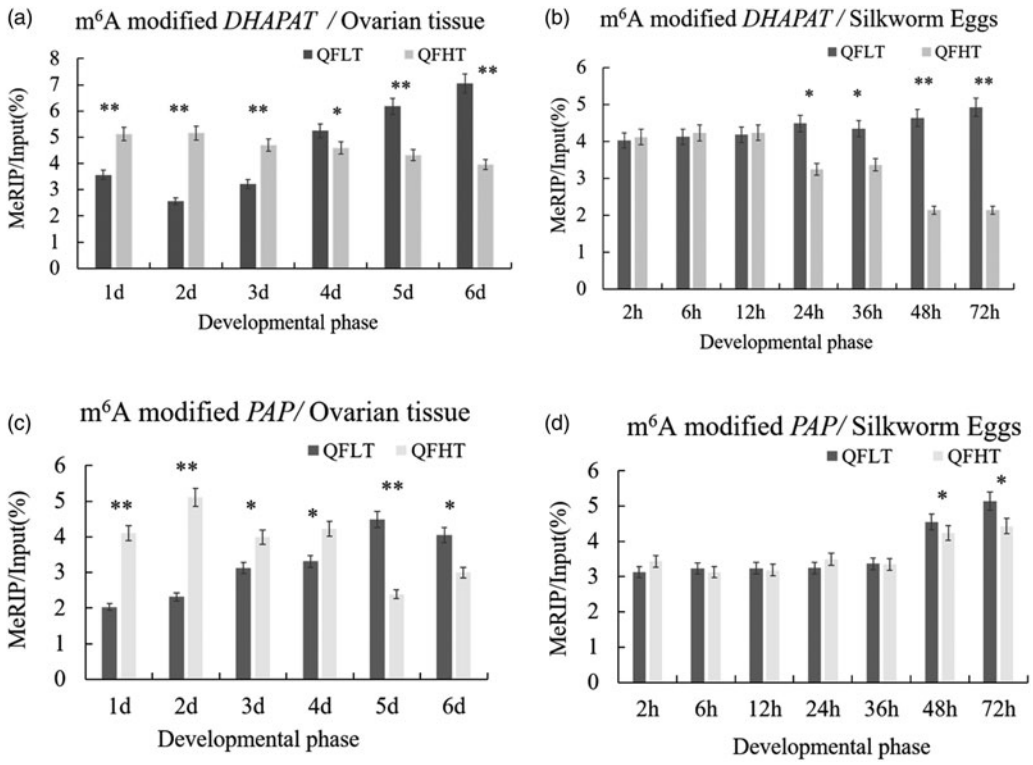

Figure 3. Expression profile of m^{6}A modified *DHAPAT* and *PAP* in QFHT and QFLT. (a) and (b) m^{6}A modified *DHAPAT* expression level in the ovary during pupa and eggs of early embryonic stage. (c) and (d) Expression level of m^{6}A modified *PAP* in the ovary during pupa and eggs of early embryonic stage. Values are mean ± SD of $n = 4$ independent experiments. ***$P < 0.001$; **$P < 0.01$; two-tailed Student's *t*-test.

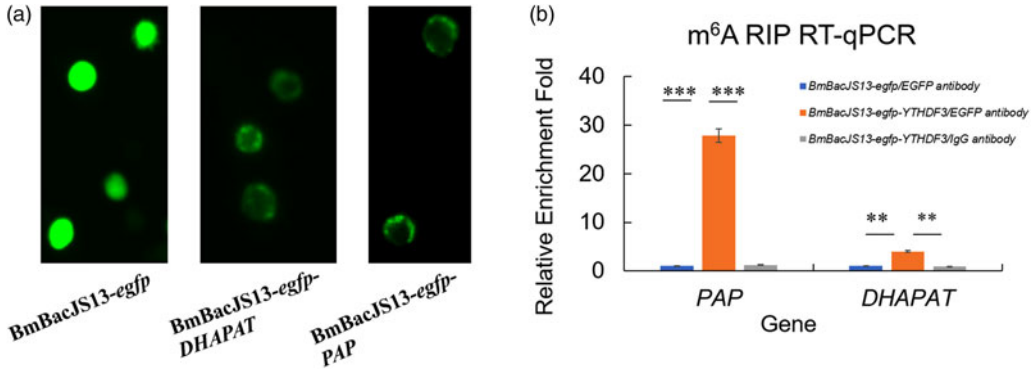

Figure 4. YTHDF3 recognizes and binds to m^{6}A modified *DHAPAT* and *PAP*. (a) Localization of BmBacJS13-*egfp*, BmBacJS13-*egfp-DHAPAT* and BmBacJS13-*egfp-PAP* in BmN cells. (b) Effect of overexpressing *YTHDF3* and *egfp* on m^{6}A modified *PAP* and *DHAPAT* by RNA immunoprecipitation (RIP) and RT-qPCR. Values are mean ± SD of $n = 4$ independent experiments. *$P < 0.05$; **$P < 0.01$; two-tailed Student's *t*-test.

Then, double luciferase reporter plasmids for the m^{6}A wt and A-T mutant were constructed according to the schematic diagram in fig. 5d. The plasmids were transfected into BmN cells for the luciferase activity assay. The luciferase activity of wt *PAP* was significantly higher than that of mutated *PAP* and the two control groups (fig. 6b). RT-qPCR showed that mRNA expression of *PAP* in the wt and mutated groups was significantly higher than that in the two groups (fig. 6c). It has been confirmed that YTHDF3 increases *PAP* stability and promotes its translation.

Discussion

Diapause is a complex insect biological characteristic, and environment-induced epigenetics play an important role in regulating, accumulating and transforming nutrients during this process(Reynolds and Hand, 2009; Reynolds *et al.*, 2019). However, the complex and diverse mechanisms of these metabolites in diapause regulation are still being uncovered. In our study, we validated that m^{6}A modification-related genes in the lipid metabolism pathway regulate diapause traits in the bivoltine strain of *B. mori*. The m^{6}A methylation rate of *DHAPAT* and *PAP* in the ovary and fat body tissue of pupae and eggs in the early embryonic stage after oviposition was higher in the non-diapausing QFLT group than in the diapausing QFHT group. *DHAPAT* knockdown in the lipid metabolism pathway in QFLT resulted in non-diapause destined eggs becoming diapause destined eggs, while knockdown of *PAP*, a downstream gene in the lipid metabolism pathway, induced a colour change in non-diapause destined

https://doi.org/10.1017/S0007485323000330 Published online by Cambridge University Press

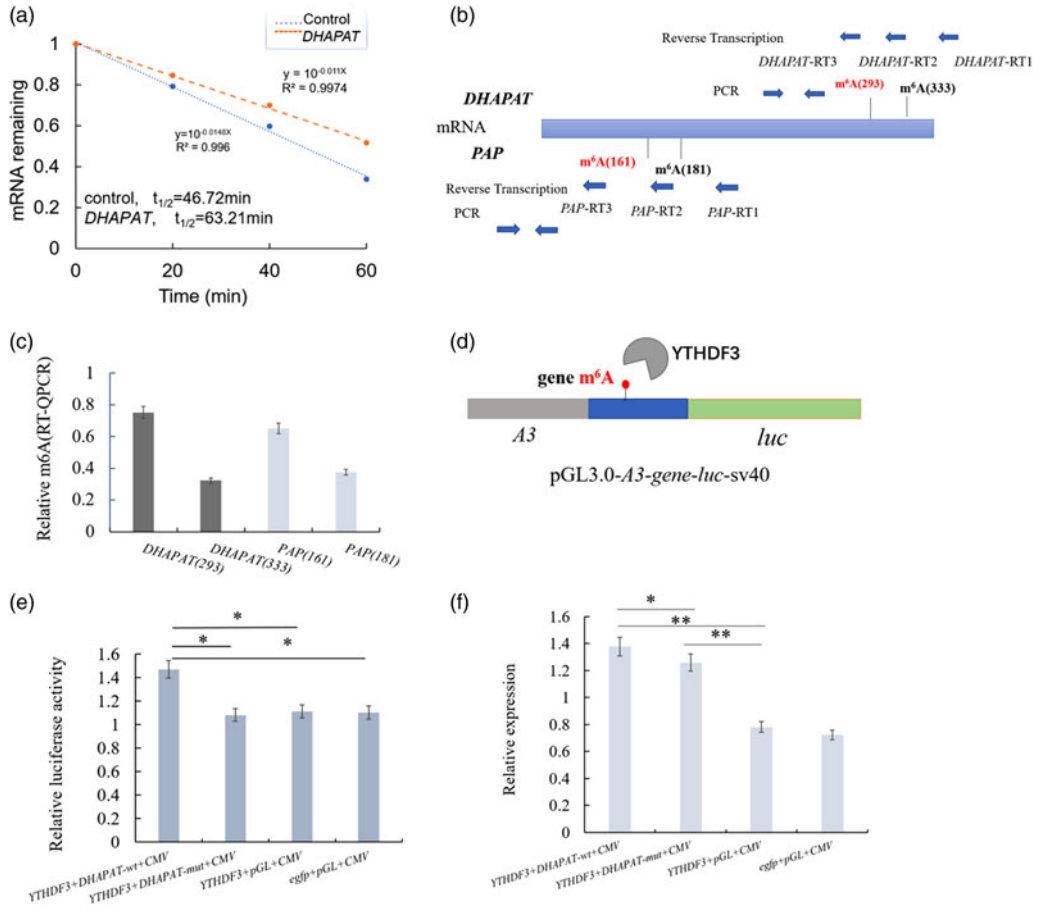

Figure 5. YTHDF3 promotes *DHAPAT* mRNA translation. (a) Overexpressing YTHDF3 increases the *DHAPAT* mRNA half-life in BmN cells. (b) Graphical representation of m^{6}A site of *DHAPAT* and *PAP*. (c) m^{6}A levels of *DHAPAT* and *PAP* in BmN cells. (d) Structure of the dual-luciferase reporter assay vector. (e) and (f) Relative firefly luciferase (Fluc) activity (protein level) and *DHAPAT* mRNA level of *DHAPAT-wt*/*DHAPAT-mut*/blank control reporters in BmN cells with overexpressing *YTHDF3*. Values are mean ± SD of $n = 4$ independent experiments. Two-tailed Student's *t*-tests were used (**$P < 0.01$, *$P < 0.05$).

eggs from light yellow to pink 3 days after oviposition, but they hatched normal non-diapausing eggs, indicating an increase in 3-hydroxycanine expression. In addition, the reader YTHDF3 recognized the m^{6}A methylation sites of *DHAPAT* and *PAP*, increasing stability and promoting their translation. m^{6}A methylation mediated the change in expression levels of *DHAPAT* and *PAP* and affected the diapause traits of bivoltine *B. mori* through the lipid metabolism pathway and tricarboxylic acid cycle. These results demonstrated that m^{6}A methylation of epigenetic modification plays an important role in regulating the expression level of *DHAPAT* and *PAP* in the lipid metabolism pathway in response to diapause-induced environmental signals and has a certain correlation with the control of the basic energy demand for the preparation and maintenance of diapause in bivoltine *B. mori*.

Epigenetics are systematic regulatory processes that have biological functions and can cooperate in all insect development stages (Stoll *et al.*, 2018). Epigenetic processes, such as histone modification, DNA methylation and non-coding RNA, have been involved in insect diapause regulation (Li *et al.*, 2019; George and Palli, 2020; Duan *et al.*, 2022). Research on RNA methylation modification is very limited to insect diapause regulation. It has been reported that histone deacetylation participates in the regulation of juvenile hormone and metamorphosis and in the development of insects (George *et al.*, 2019; George and Palli, 2020). Interference by miR-277-3p in *Aedes aegypti* activates insulin signalling to enhance the nuclear output of *FOXO*, leading to the failure of lipid storage and ovarian development (Ling *et al.*, 2017). Diapausing and non-diapausing *Culex pipiens* showed significant differences in the expression of several miRNAs related to lipid metabolism in the fat body and ovary, and the change in miRNA abundance was related to the phenotypic change in diapause (Meuti *et al.*, 2018). This shows that epigenetic modification interacts with lipid metabolism signals to affect the diapause fate in insects, but the response mechanism of m^{6}A modification coupling lipid metabolism to the diapause-induced environment is still not completely clarified.

We also showed that the m^{6}A methylation levels were significantly different between non-diapause destined and diapause destined bivoltine *B. mori*. However, the complicated regulation network of the *B. mori* diapause mechanism with epigenetic involvement is deficient. The function of a specific gene in the diapause phenotype depends on its expression abundance and tissue specificity, as well as its upstream and downstream regulatory pathways (Reynolds *et al.*, 2017; Sahoo *et al.*, 2018). In particular, lipids are the main nutrients for diapause insects to cope with energy deprivation, and their accumulation and utilization mechanisms are complex and diverse (Vukašinović *et al.*, 2015; Batz and Armbruster, 2018). Studies have shown that epigenetic modification mainly affects the splicing, transport, stability and translation efficiency of RNA mediated by a series of reader

https://doi.org/10.1017/S0007485323000330 Published online by Cambridge University Press

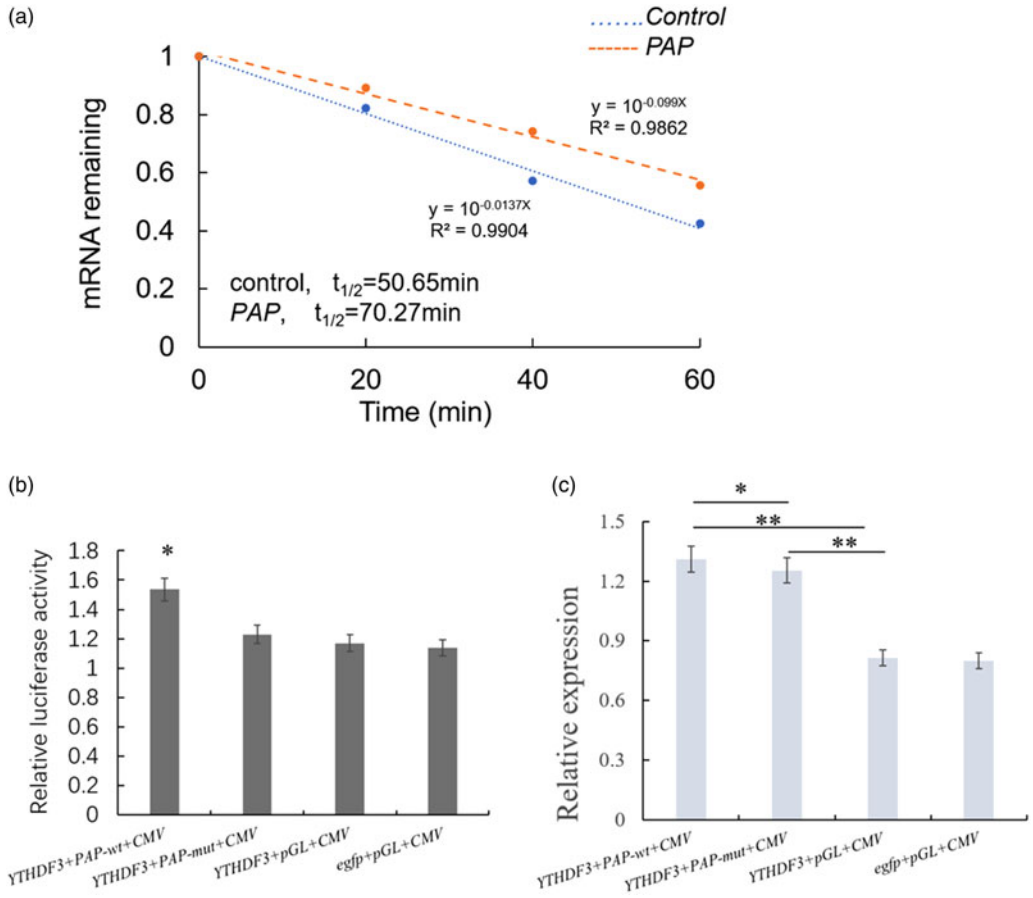

Figure 6. YTHDF3 promotes *PAP* mRNA translation. (a) Overexpressing YTHDF3 increases the *PAP* mRNA half-life. (b) and (c) Relative firefly luciferase activity (protein level) and *PAP* mRNA level of *PAP-wt*/*PAP-mut*/blank control reporters in BmN cells with overexpressing *YTHDF3*. Values are mean ± SD of $n = 4$ independent experiments. Two-tailed Student's *t*-tests were used (**$P < 0.01$, *$P < 0.05$).

proteins (Dominissini *et al.*, 2012; Du *et al.*, 2016; Slobodin *et al.*, 2017). A typical feature of diapause is that the gene expression level is widely downregulated (Denlinger, 2002). In this experiment, a higher m^{6}A methylation modification rate of *DHAPAT* and *PAP* in the ovary and early embryos of the QFLT group than in the QFHT group may be conducive to recognition and translation mediated by YTHDF3, suggesting that the increased expression abundance of these two genes can promote lipid metabolism in QFLT and provide more energy for embryo development.

In summary, our experimental results showed that the environmental signals, such as temperature and photoperiod, received during the parental embryo period of bivoltine *B. mori* changed the m^{6}A RNA modification level of some genes, thus affecting YTHDF3 expression (higher expression level in pupae from eggs incubated under a low temperature in the dark and low expression level in pupae from eggs incubated under a normal temperature in a natural light cycle). A higher level of YTHDF3 promotes the expression of m^{6}A-modified *DHAPAT* and *PAP* genes (including m^{6}A modification abundance, mRNA stability and translation) in the pupal stage to provide energy for embryo development, resulting in offspring eggs developing being non-diapausing; otherwise, the offspring are diapausing. These results indicate that m^{6}A methylation mediates the regulation of environmental signals in the diapause of bivoltine *B. mori*. Taken together, the results partly explain the molecular mechanism of bivoltine *B. mori* diapause changes induced by environmental signals, which provides a reference for studying the relationship between lipid metabolism and diapause and a new target for controlling pests in agriculture and forestry.

Acknowledgements. This work was supported by the National Natural Science Foundation of China (Grant No. 32072791 and No. 32102609) and the Postgraduate Research & Practice Innovation Program of Jiangsu Province (No. KYCX21_3508)

Author contributions. Y.-H. C., T. J. and X.-J. S. led the experiments and designed the analytical strategy; Y.-H. C., A. Y. and B.-Y. F. performed the experiments; Y.-H. C., T. J., J. Z., M.-X. W. and X.-J.-S. analysed the data; Y.-H. C. and X.-J. S. wrote the manuscript. All authors have made a contribution to the final manuscript, and have read and approved the final manuscript.

Conflict of interest. None.

Data availability statement. All data are contained within the article.

References

Amsalem E, Galbraith D, Cnaani J, Teal P and Grozinger C (2015) Conservation and modification of genetic and physiological toolkits underpinning diapause in bumble bee queens. *Molecular Ecology* **24**, 5596–5615.

Arrese EL and Soulages JL (2009) Insect fat body: energy, metabolism, and regulation. *Annual Review of Entomology* **55**, 207–225.

Batz ZA and Armbruster PA (2018) Diapause-associated changes in the lipid and metabolite profiles of the Asian tiger mosquito, *Aedes albopictus*. *Journal of Experimental Biology* **221**, jeb189480.

https://doi.org/10.1017/S0007485323000330 Published online by Cambridge University Press

Batz ZA, Goff AC and Armbruster PA (2017) MicroRNAs are differentially abundant during *Aedes albopictus* diapause maintenance but not diapause induction. *Insect Molecular Biology* **26**, 721–733.

Boissel S, Reish O, Proulx K, Kawagoe-Takaki H, Sedgwick B, Yeo GS, Meyre D, Golzio C, Molinari F, Kadhom N, Etchevers HC, Saudek V, Farooqi IS, Froguel P, Lindahl T, O'Rahilly S, Munnich A and Colleaux L (2009) Loss-of-function mutation in the dioxygenase-encoding FTO gene causes severe growth retardation and multiple malformations. *American Journal of Human Genetics* **85**, 106–111.

Bonasio R, Tu S and Reinberg D (2010) Molecular signals of epigenetic states. *Science* **330**, 612–616.

Castellanos-Rubio A, Santin I, Olazagoitia-Garmendia A, Romero-Garmendia I, Jauregi-Miguel A, Legarda M and Bilbao JR (2019) A novel RT-QPCR-based assay for the relative quantification of residue specific m6A RNA methylation. *Scientific Reports* **9**, 4220.

Chen Y, Fan B, Yasen A, Zhu J, Wang M and Shen X (2022) YTHDF3 is involved in the diapause process of bivoltine *Bombyx mori* strains by regulating the expression of Cyp307a1 and Cyp18a1 genes in the ecdysone synthesis pathway. *Biomolecules* **12**, 1127.

Chen YH, Jiang T, Yasen A, Fan BY, Zhu J, Wang MX, Qian P and Shen XJ (2023) m(6)A-dependent mevalonate kinase in juvenile hormone synthesis pathway regulates the diapause process of bivoltine silkworm (*Bombyx mori*). *Molecular Biology Reports* **50**, 5295–5306.

Denlinger DL (2002) Regulation of diapause. *Annual Review of Entomology* **47**, 93–122.

Dominissini D, Moshitch-Moshkovitz S, Schwartz S, Salmon-Divon M, Ungar L, Osenberg S, Cesarkas K, Jacob-Hirsch J, Amariglio N, Kupiec M, Sorek R and Rechavi G (2012) Topology of the human and mouse m6A RNA methylomes revealed by m6A-seq. *Nature* **485**, 201–206.

Du H, Zhao Y, He J, Zhang Y, Xi H, Liu M, Ma J and Wu L (2016) YTHDF2 destabilizes m(6)A-containing RNA through direct recruitment of the CCR4-NOT deadenylase complex. *Nature Communications* **7**, 12626.

Duan T-F, Li L, Wang H-C and Pang B-P (2022) MicroRNA miR-2765-3p regulates reproductive diapause by targeting FoxO in *Galeruca daurica*. *Insect Science* **30**, 279–292.

Fischman BJ, Pitts-Singer TL and Robinson GE (2017) Nutritional regulation of phenotypic plasticity in a solitary bee (Hymenoptera: Megachilidae). *Environmental Entomology* **46**, 1070–1079.

Gebeyew K, Yang C, Mi H, Cheng Y, Zhang T, Hu F, Yan Q, He Z, Tang S and Tan Z (2022) Lipid metabolism and m(6)A RNA methylation are altered in lambs supplemented rumen-protected methionine and lysine in a low-protein diet. *Journal of Animal Science and Biotechnology* **13**, 85.

George S and Palli SR (2020) Histone deacetylase 11 knockdown blocks larval development and metamorphosis in the red flour beetle, *Tribolium castaneum*. *Frontiers in Genetics* **11**, 683.

George S, Gaddelapati SC and Palli SR (2019) Histone deacetylase 1 suppresses Krüppel homolog 1 gene expression and influences juvenile hormone action in *Tribolium castaneum*. *PNAS* **116**, 17759–17764.

Gupta A.P. (1991) Morphogenetic hormones of arthropodss. In Schooneveld H (ed.), *ecent Advances In Comparative Arthropod Morphology, Physiology, And Development*, Vol. 3. New Brunswick: Rutgers University Press.

Hahn DA and Denlinger DL (2007) Meeting the energetic demands of insect diapause: nutrient storage and utilization. *Journal of Insect Physiology* **53**, 760–773.

Hand SC, Menze MA, Borcar A, Patil Y, Covi JA, Reynolds JA and Toner M (2011) Metabolic restructuring during energy-limited states: insights from *Artemia franciscana* embryos and other animals. *Journal of Insect Physiology* **57**, 584–594.

Izumi Y, Sonoda S and Tsumuki H (2007) Effects of diapause and cold-acclimation on the avoidance of freezing injury in fat body tissue of the rice stem borer, *Chilo suppressalis* Walker. *Journal of Insect Physiology* **53**, 685–690.

Jiang T, Li J, Qian P, Xue P, Xu J, Chen Y, Zhu J, Shunming T, Zhao Q, Qian H and Shen X-J (2019) The role of N6-methyladenosine modification on diapause in silkworm (*Bombyx mori*) strains that exhibit different voltinism. *Molecular Reproduction and Development* **86**, 1981–1992.

Kang DS, Cotten MA, Denlinger DL and Sim C (2016) Comparative transcriptomics reveals key gene expression differences between diapausing and non-diapausing adults of *Culex pipiens*. *PLoS ONE* **11**, e0154892.

Kitagawa N, Shiomi K, Imai K, Niimi T, Yaginuma T and Yamashita O (2005) Establishment of a sandwich ELISA system to detect diapause hormone, and developmental profile of hormone levels in egg and subesophageal ganglion of the silkworm, *Bombyx mori*. *Zoological Science* **22**, 213–221.

Koštál V (2006) Eco-physiological phases of insect diapause. *Journal of Insect Physiology* **52**, 113–127.

Lehmann P, Pruisscher P, Posledovich D, Carlsson M, Käkelä R, Tang P, Nylin S, Wheat CW, Wiklund C and Gotthard K (2016) Energy and lipid metabolism during direct and diapause development in a pierid butterfly. *Journal of Experimental Biology* **219**, 3049–3060.

Li Y, Zhang L, Chen H, Koštál V, Simek P, Moos M and Denlinger DL (2015) Shifts in metabolomic profiles of the parasitoid *Nasonia vitripennis* associated with elevated cold tolerance induced by the parasitoid's diapause, host diapause and host diet augmented with proline. *Insect Biochemistry and Molecular Biology* **63**, 34–46.

Li B, Hu P, Zhang SZ, Toufeeq S, Wang J, Zhao K, Xu X, Xu JP and Huang SJ (2019) DNA methyltransferase BmDnmt1 and BmDnmt2 in silkworm (*Bombyx mori*) and the regulation of silkworm embryonic development. *Archives of Insect Biochemistry and Physiology* **100**, e21529.

Li B, Hu P, Zhu LB, You LL, Cao HH, Wang J, Zhang SZ, Liu MH, Toufeeq S, Huang SJ and Xu JP (2020) DNA methylation is correlated with gene expression during diapause termination of early embryonic development in the silkworm (*Bombyx mori*). *International Journal of Molecular Sciences* **21**, 671.

Ling L, Kokoza VA, Zhang C, Aksoy E and Raikhel AS (2017) MicroRNA-277 targets insulin-like peptides 7 and 8 to control lipid metabolism and reproduction in *Aedes aegypti* mosquitoes. *PNAS* **114**, E8017–e8024.

Meister P, Schott S, Bedet C, Xiao Y, Rohner S, Bodennec S, Hudry B, Molin L, Solari F, Gasser SM and Palladino F (2011) *Caenorhabditis elegans* heterochromatin protein 1 (HPL-2) links developmental plasticity, longevity and lipid metabolism. *Genome Biology* **12**, R123.

Meuti ME, Bautista-Jimenez R and Reynolds JA (2018) Evidence that microRNAs are part of the molecular toolkit regulating adult reproductive diapause in the mosquito, *Culex pipiens*. *PLoS ONE* **13**, e0203015.

Pitts-Singer TL (2020) Photoperiod effect on *Megachile rotundata* (Hymenoptera: Megachilidae) female regarding diapause status of progeny: the importance of data scrutiny. *Environmental Entomology* **49**, 516–527.

Popović ŽD, Subotić A, Nikolić TV, Radojičić R, Blagojević DP, Grubor-Lajšić G and Koštál V (2015) Expression of stress-related genes in diapause of European corn borer (*Ostrinia nubilalis* Hbn.). *Comparative Biochemistry and Physiology Part B: Biochemistry and Molecular Biology* **186**, 1–7.

Poupardin R, Schöttner K, Korbelová J, Provazník J, Dolezel D, Pavlinic D, Beneš V and Kostál V (2015) Early transcriptional events linked to induction of diapause revealed by RNAseq in larvae of drosophilid fly, *Chymomyza costata*. *BMC Genomics* **16**, 720.

Ragland GJ and Keep E (2017) Comparative transcriptomics support evolutionary convergence of diapause responses across Insecta. *Physiological Entomology* **42**, 246–256.

Ragland GJ, Denlinger DL and Hahn DA (2010) Mechanisms of suspended animation are revealed by transcript profiling of diapause in the flesh fly. *PNAS* **107**, 14909–14914.

Rando OJ (2012) Daddy issues: paternal effects on phenotype. *Cell* **151**, 702–708.

Reynolds JA (2017) Epigenetic Influences on Diapause. *Advances in Insect Physiology* **53**, 115–144.

Reynolds JA and Hand SC (2009) Embryonic diapause highlighted by differential expression of mRNAs for ecdysteroidogenesis, transcription and lipid sparing in the cricket *Allonemobius socius*. *Journal of Experimental Biology* **212**, 2075–2084.

Reynolds JA, Poelchau MF, Rahman Z, Armbruster PA and Denlinger DL (2012) Transcript profiling reveals mechanisms for lipid conservation during diapause in the mosquito, *Aedes albopictus*. *Journal of Insect Physiology* **58**, 966–973.

https://doi.org/10.1017/S0007485323000330 Published online by Cambridge University Press

Reynolds JA, Peyton JT and Denlinger DL (2017) Changes in microRNA abundance may regulate diapause in the flesh fly, *Sarcophaga bullata*. *Insect Biochemistry and Molecular Biology* **84**, 1–14.

Reynolds JA, Nachman RJ and Denlinger DL (2019) Distinct microRNA and mRNA responses elicited by ecdysone, diapause hormone and a diapause hormone analog at diapause termination in pupae of the corn earworm, *Helicoverpa zea*. *General and Comparative Endocrinology* **278**, 68–78.

Sahoo A, Dutta A, Dandapat J and Samanta L (2018) Low H2O2 and enhanced oxidative resistance in the diapause-destined pupa of silkworm, *Antheraea mylitta* (Lepidoptera:Saturniidae) suggest their possible involvement in dormancy and lifespan extension. *BMC Zoology* **3**, 1.

Slobodin B, Han R, Calderone V, Vrielink J, Loayza-Puch F, Elkon R and Agami R (2017) Transcription impacts the efficiency of mRNA translation via co-transcriptional N6-adenosine methylation. *Cell* **169**, 326–337, e312.

Smemo S, Tena JJ, Kim KH, Gamazon ER, Sakabe NJ, Gómez-Marín C, Aneas I, Credidio FL, Sobreira DR, Wasserman NF, Lee JH, Puviindran V, Tam D, Shen M, Son JE, Vakili NA, Sung HK, Naranjo S, Acemel RD, Manzanares M, Nagy A, Cox NJ, Hui CC, Gomez-Skarmeta JL and Nóbrega MA (2014) Obesity-associated variants within FTO form long-range functional connections with IRX3. *Nature* **507**, 371–375.

Stoll S, Wang C and Qiu H (2018) DNA methylation and histone modification in hypertension. *International Journal of Molecular Sciences* **19**, 703–715.

Süess P, Dircksen H, Roberts KT, Gotthard K, Nässel DR, Wheat CW, Carlsson MA and Lehmann P (2022) Time- and temperature-dependent dynamics of prothoracicotropic hormone and ecdysone sensitivity co-regulate pupal diapause in the green-veined white butterfly *Pieris napi*. *Insect Biochemistry and Molecular Biology* **149**, 103833.

Takemoto S, Nakano M, Fukami T and Nakajima M (2021) m(6)A modification impacts hepatic drug and lipid metabolism properties by regulating carboxylesterase 2. *Biochemical Pharmacology* **193**, 114766.

Taylor LR (1987) Review of Seasonal Adaptations of Insects. *Journal of Animal Ecology* **56**, 374–375.

Vukašinović EL, Pond DW, Worland MR, Kojić D, Purać J, Popović Ž D and Grubor-Lajšić G (2015) Diapause induces remodeling of the fatty acid composition of membrane and storage lipids in overwintering larvae of *Ostrinia nubilalis*, Hubn. (Lepidoptera: Crambidae). *Comparative Biochemistry and Physiology Part B: Biochemistry and Molecular Biology* **184**, 36–43.

Vukašinović EL, Pond DW, Grubor-Lajšić G, Worland MR, Kojić D, Purać J, Popović ŽD and Blagojević DP (2018) Temperature adaptation of lipids in diapausing *Ostrinia nubilalis*: an experimental study to distinguish environmental versus endogenous controls. *Journal of Comparative Physiology B* **188**, 27–36.

Wadsworth C and Dopman E (2015) Transcriptome profiling reveals mechanisms for the evolution of insect seasonality. *Journal of Experimental Biology* **218**, 3611–3622.

Wang X, Zhu L, Chen J and Wang Y (2015) mRNA m6A methylation downregulates adipogenesis in porcine adipocytes. *Biochemical and Biophysical Research Communications* **459**, 201–207.

Wang Y, Wang Y, Gu J, Su T, Gu X and Feng Y (2022) The role of RNA m6A methylation in lipid metabolism. *Frontiers in Endocrinology* **13**, 866116.

Zhong X, Yu J, Frazier K, Weng X, Li Y, Cham CM, Dolan K, Zhu X, Hubert N, Tao Y, Lin F, Martinez-Guryn K, Huang Y, Wang T, Liu J, He C, Chang EB and Leone V (2018) Circadian clock regulation of hepatic lipid metabolism by modulation of m6A mRNA methylation. *Cell Reports* **25**, 1816–1828, e1814.

https://doi.org/10.1017/S0007485323000330 Published online by Cambridge University Press